

CXCR3 deficiency enhances tumor progression by promoting macrophage M2 polarization in a murine breast cancer model

Steve Oghumu,^{1,2} Sanjay Varikuti,¹
Cesar Terrazas,¹ Dmitri Kotov,¹
Mohd W. Nasser,¹ Catherine A.
Powell,¹ Ramesh K. Ganju¹ and
Abhay R. Satoskar¹

¹Department of Pathology, The Ohio State University Medical Center, Columbus, OH, and ²Department of Oral Biology, The Ohio State University College of Dentistry, Columbus, OH, USA

doi:10.1111/imm.12293

Received 24 August 2013; revised 12 March 2014; accepted 24 March 2014.

Correspondence: Dr Abhay R. Satoskar, Department of Pathology, 1645 Neil Avenue Columbus, Ohio 43210, USA.

Email: abhay.satoskar@osumc.edu

Senior author: Dr Abhay R. Satoskar

Introduction

Tumor associated immune cells together with their state of activation and differentiation play a major role in determining the outcome of a majority of human cancers of the breast and other tissues.^{1,2} The presence of Th1 cells, NK cells and cytotoxic CD8 cells within the tumor microenvironment is generally associated with regression of tumors and a favorable prognosis.^{1,3} In contrast, infiltration by Th2 cells, Tregs and B cells promote tumor development and disease progression.⁴ Tumor associated macrophages (TAMs) generally differentiate into alternatively activated (M2) phenotypes in response to distinct

Summary

Tumor associated macrophages play a vital role in determining the outcome of breast cancer. We investigated the contribution of the chemokine receptor CXCR3 to antitumor immune responses using a *cxcr3* deficient mouse orthotopically injected with a PyMT breast cancer cell line. We observed that *cxcr3* deficient mice displayed increased IL-4 production and M2 polarization in the tumors and spleens compared to WT mice injected with PyMT cells. This was accompanied by larger tumor development in *cxcr3*^{-/-} than in WT mice. Further, tumor-promoting myeloid derived immune cell populations accumulated in higher proportions in the spleens of *cxcr3* deficient mice. Interestingly, *cxcr3*^{-/-} macrophages displayed a deficiency in up-regulating inducible nitric oxide synthase after stimulation by either IFN- γ or PyMT supernatants. Stimulation of bone marrow derived macrophages by PyMT supernatants also resulted in greater induction of arginase-1 in *cxcr3*^{-/-} than WT mice. Further, *cxcr3*^{-/-} T cells activated with CD3/CD28 *in vitro* produced greater amounts of IL-4 and IL-10 than T cells from WT mice. Our data suggests that a greater predisposition of *cxcr3* deficient macrophages towards M2 polarization contributes to an enhanced tumor promoting environment in *cxcr3* deficient mice. Although CXCR3 is known to be expressed on some macrophages, this is the first report that demonstrates a role for CXCR3 in macrophage polarization and subsequent breast tumor outcomes. Targeting CXCR3 could be a potential therapeutic approach in the management of breast cancer tumors.

Keywords: arginase-1; breast cancer; CXCR3; inducible nitric oxide synthase; tumor associated macrophages.

signals within the tumor environment (such as IL-4, IL-10, IL-13, TGF- β , M-CSF), which in turn contribute to tumor growth and progression.^{2,5-7} Understanding the mechanisms that direct the activation and differentiation of immune cell populations in response to a tumor challenge will provide a basis for novel cancer therapeutic strategies.

The chemokine receptor CXCR3 has long been known to contribute to the migration, activation and differentiation of a number of immune cells, and has been shown to play a major role in a wide range of infectious, autoimmune and neoplastic diseases.⁸⁻¹⁴ CXCR3 is expressed by Th1 cells, cytotoxic CD8 T cells, NK and NKT cells and it

Abbreviations: PyMT, Polyoma Middle T; IL, Interleukin; TAM, Tumor associated Macrophage; IFN, Interferon

has been shown to be involved in their activation. It is regulated by the transcription factor T-bet and therefore generally considered a canonical marker for Th1 cells.¹⁵ As a chemokine receptor, CXCR3 mediates the recruitment of effector cells to inflammatory sites and is essential for the resolution of a number of infectious diseases that require a Th1 immune response for protection.^{9,10,12}

In the context of cancer, reports on the role of CXCR3 appear to be conflicting. In some murine breast cancer models, expression of CXCR3 has been associated with poor prognosis and metastasis of tumor cells.^{16,17} In other models, migration of tumor infiltrating NK cells and effector T cells to tumor sites require the expression of CXCR3 ligands MIG and IP-10, resulting in tumor suppression and control of metastasis.^{18,19} This has led some researchers to explore therapeutic strategies which involve stimulating the production of these ligands in human breast cancer.²⁰

CXCR3 is also expressed in macrophages,^{21–23} and a few reports have demonstrated a requirement for CXCR3 in the recruitment and activation of macrophages in some animal disease models.^{24–26} However, not much is known about the role CXCR3 plays in the recruitment and activation of TAMs in murine breast cancer models. Although classically activated M1 macrophages possess tumoricidal activity, majority of TAMs in solid tumors are characterized as alternatively activated M2 macrophages, which have been shown to contribute to tumor progression and poor prognosis in cancer patients.²⁷ The molecular mechanisms and factors that determine the presence and activation state of TAMs within breast cancer tumors are still not completely understood.

It is evident that the role for CXCR3 in breast cancer is complex and dependent on a number of factors including cancer type, stage of disease and the interactions between CXCR3 expressing cells within the tumor microenvironment. In this study, we examine the role of CXCR3 in an orthotopic breast cancer murine model using *cxcr3*^{-/-} mice injected with a breast cancer cell line derived from an MMTV-PyMT transgenic mouse. We provide evidence that the absence of CXCR3 contributes to enhanced growth and progression of breast cancer tumors as well as increased levels of tumor enhancing immune cells and host factors.

Materials and methods

Mice, cell lines and cancer injection protocol

C57BL/6 mice and *cxcr3*^{-/-} mice were maintained at the Ohio State University animal facility according to animal protocols and University Laboratory Animal Resources (ULAR) regulations. All experiments were approved by the Institutional Animal Care and Use Committee (IACUC) and Institutional Biosafety Committee (IBC) of the Ohio State University. Polyoma Middle T (PyMT) encoded

breast cancer cell lines (derived from C57BL/6 MMTV-PyMT mice) were kindly provided by Dr. Hai²⁸ at The Ohio State University Medical Center and maintained in DMEM-F12 cell culture media (Invitrogen, Carlsbad, CA). One million PyMT cells were injected into the mammary glands (# 4) of 6 week old female WT and *cxcr3*^{-/-} mice. Animals were monitored daily for 6–7 weeks and animals were sacrificed at the end of the 7 week period or until tumors met the requirements for a humane endpoint.

Tumor measurements

Tumor growth was monitored weekly for 7 weeks and measured using digital calipers to determine the widths and lengths of the tumor. Tumor volumes were determined by the formula $0.52 \times a \times b^2$, where *a* and *b* are the long and short diameters of the tumors respectively.²⁹ Mice having tumors with diameters between 1.5 and 2 cm were sacrificed as an experimental endpoint according to the animal protocol.

Flow cytometry

Single cell suspensions were prepared from spleens and tumors of WT and *cxcr3*^{-/-} mice, washed with PBS and blocked with normal mouse serum or anti CD16/CD32 antibodies. Cells were incubated with conjugated antibodies against various cell surface markers including CD4, CD8, CD3, NK1-1, F4/80, CD206 and CD11b (Biolegend, San Diego, CA). Cells were acquired on a BD FACS Calibur (BD Biosciences, San Jose, CA) and analysis was performed with FlowJo software (Tree Star, Inc., Ashland, OR).

Real-time PCR analysis

Total RNA from spleens and tumors were extracted using TRIzol reagent (Invitrogen). RNA concentration was determined by absorbance at 260 nm. One microgram RNA was used for first strand cDNA synthesis with SuperScript VILO cDNA synthesis kit (Invitrogen). Primer sequences and cycling conditions for real-time PCR were obtained using the Harvard Medical School's PRIMER BANK website (<http://pga.mgh.harvard.edu/primerbank/index.html>). PCR amplification was performed in an Opticon Real-Time PCR cycler (Biorad, Hercules, CA) using SYBR Green (BioRad) for detection. Data were normalized to β -actin and presented as fold induction over unstimulated cells using the $\Delta\Delta C_T$ method.

Histology and immunohistochemistry

Tumors from WT and *cxcr3*^{-/-} mice were either formalin fixed tissue embedded (FFPE) or cryopreserved in OCT medium for histological analysis and immunohistochemistry. For histological analysis, FFPE sections were stained with

H&E and slides were examined under a Zeiss light microscope. For immunohistochemistry, cryosections were stained with arginase-1 (Santa Cruz Biotechnology Inc, Santa Cruz, CA 1 : 200), and rabbit anti-mouse inducible nitric oxide synthase (iNOS; Abcam, Cambridge, MA 1 : 200) for 60 min at room temperature. Vectastain Elite ABC reagents (Vector Laboratories, Burlingame, CA), using avidin DH:biotinylated horseradish peroxidase H complex with 3,3'-diaminobenzidine (Polysciences, Warrington, PA) and Mayer's hematoxylin (Fisher Scientific, Pittsburgh, PA), were used for detection of the bound antibodies.

In vitro T cell activation

Single cell suspensions were obtained from excised lymph nodes and spleens of naive WT and *cxcr3*^{-/-} mice. Splenocytes were incubated with Boyle's solution at room temp for 10 min to lyse red blood cells then washed with RPMI supplemented with 10%FBS. Enriched T cell populations were obtained by passing cell suspensions through nylon wool columns. Cells were incubated at 0.5–2.5 × 10⁶ cells/well with plate bound anti-CD3 (3 µg/ml, clone 145–2C11) and anti-CD28 (4 µg/ml, clone 37.51) Abs (Biolegend) for 48, 72 and 96 hr. Following *in vitro* activation, culture supernatants were analyzed for cytokine production using ELISA.

Cytokine ELISA

Cytokine ELISAs were performed on culture supernatants of *in vitro* activated BMDMs. Briefly, purified anti-mouse IL-6, IL-10, IL-12 and TNF-α monoclonal antibodies (Biolegend) were used as capture antibodies for each respective ELISA. Recombinant mouse IL-6, IL-10, IL-12 and TNF-α (BD pharmingen, San jose, CA) were used as standards. Detection of cytokines was performed using biotinylated anti-mouse antibodies (Biolegend), streptavidin conjugated alkaline phosphatase (BD pharmingen) and p-nitrophenyl phosphate (PNPP) (ThermoFisher Scientific, Pittsburg, PA) as substrate. Plates were read using Spectramax Mmicroplate reader (Molecular Devices LLC, Sunnyvale, CA) at an absorbance of 405 nm. Cytokine concentrations were determined by extrapolating from the generated standard curve using Softmax Pro software (Molecular Devices LLC).

Generation and stimulation of bone marrow derived macrophages

Single cell suspensions were prepared from bones of C57BL/6 and *cxcr3*^{-/-} mice. After red blood cell (RBCs) lysis with ACK lysis buffer, BMDMs were generated by incubating cells with 2% Colony Stimulating Factor (CSF), 10% FBS, 1% Pen-Strep and 1% HEPES in RPMI 1640 media at 37° with 5% CO₂ for about 72 hr.

BMDMs were stimulated with 10 ng/ml recombinant mouse IFN-γ (Roche, Indianapolis, IN), 20 ng/ml IL-4 (Roche), 1 µg/ml LPS (Sigma Aldrich, St. Louis, MO) or PyMT supernatants for 24, 48 and 72 hr. RNA was extracted from cells for real time PCR analysis and cell culture supernatants were harvested for cytokines analysis and nitric oxide production.

Nitric oxide assay

Release of nitric oxide from stimulated BMDMs in culture supernatants was determined by measurement of nitrite using Griess reagent (Sigma Aldrich) with sodium nitrite as standard. Plates were read using a Spectramax M3 microplate reader (Molecular Devices LLC) at an absorbance of 570 nm. Concentrations of nitric oxide were determined by extrapolating from the generated standard curve using Softmax Pro software (Molecular Devices LLC).

In vivo antibody injections

Cxcr3^{-/-} mice injected with PyMT cells were treated with either 1 mg rat anti IL-4 monoclonal antibody (BioXcell, West Lebanon, NH) or rat IgG isotype control (Sigma Aldrich) weekly for 5 weeks via the intra-peritoneal route. Lesions were monitored and tumor weights were determined.

Statistical analysis

Student's unpaired *t* test was used to determine statistical significance of values obtained. *P* values < 0.05 were considered statistically significant.

Results

Increased tumor growth in *cxcr3*^{-/-} mice injected with PyMT breast cancer cell line

To determine whether CXCR3 plays a role in the control of tumor progression in an *in vivo* orthotopic model of breast cancer, we injected PyMT breast cancer cells, derived from MMTV-PyMT transgenic mice, into the mammary glands of female WT and *cxcr3*^{-/-} C57BL/6 mice and followed the development of tumors daily. This cell line produces aggressive and rapidly developing tumors in C57BL/6 mice. As expected, tumors from both groups developed rapidly, but we observed that tumor volumes in *cxcr3*^{-/-} mice were significantly greater than WT mice beginning at week 2 (Fig. 1a). This was accompanied by a significant increase in the sizes of tumors from *cxcr3*^{-/-} mice (Fig. 1b). These results indicate that the absence of CXCR3 contributes increased tumor growth and progression in a PyMT orthotopic syngeneic model of breast cancer.

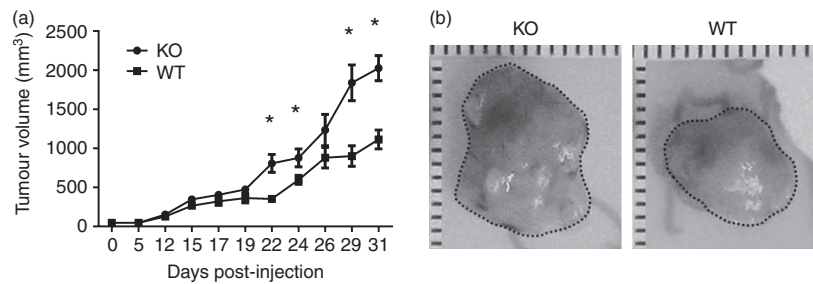


Figure 1. Increased tumor growth in *cxcr3*^{-/-} mice injected with PyMT breast cancer cell line: (a) Volumes of tumors of WT and *cxcr3*^{-/-} mice injected with PyMT cancer cell line. Measurements were taken using an external digital caliper. Data are mean values from 8 to 10 individual mice per group and are representative of three independent experiments with similar results. **P* < 0.05. (b) Representative images of tumors from WT and *cxcr3*^{-/-} mice injected with PyMT cell line.

Frequency of tumor infiltrating lymphocytes in PyMT injected WT and *cxcr3*^{-/-} C57BL/6 mice

Since tumor infiltrating lymphocytes play a role in anti-tumor immune responses to breast cancer, we analyzed the frequency of T cells in breast tumors, draining lymph nodes and spleens of mice with orthotopic PyMT breast cancer cells. We observed slightly higher numbers of tumor infiltrating CD4⁺ cells and CD8⁺ cells in WT than in *cxcr3*^{-/-} mice although differences were not statistically significant (Fig. 2a,b). In the spleens, lymphocytic populations were comparable in both groups of mice, although in the draining lymph nodes, the frequency of CD4⁺ and CD8⁺ T cells are slightly increased in *cxcr3*^{-/-} breast cancer tumor bearing mice (Fig. 2c,d). These results suggest that migration of T cells to tumor sites is slightly increased in WT mice, but is not severely impaired in *cxcr3*^{-/-} mice in the PyMT breast cancer model. To characterize the immune responses generated by these immune cell populations within the tumor microenvironment, we analyzed IL-4, IL-10 and IFN- γ mRNA levels by real time PCR. While IFN- γ levels were similar in both tumors derived from WT and *cxcr3*^{-/-} mice, levels of the Th2 cytokine IL-4 were higher in *cxcr3*^{-/-} mice group (Fig. 2e-g). Taken together these findings suggest that the migration of T cells is slightly impaired in *cxcr3*^{-/-} mice, and increased production of IL-4 by tumor infiltrating immune cells could contribute to enhanced progression of breast cancer in the PyMT orthotopic syngeneic mouse model.

M2 macrophage populations are increased in *cxcr3*^{-/-} mice containing tumors

To determine other cellular mechanisms responsible for increased tumor growth in the absence of CXCR3, we next examined various tumor associated immune cell populations involved in tumor growth of WT and *cxcr3*^{-/-} mice injected with PyMT cells. We observed similar levels of macrophage infiltration into tumor sites in WT and *cxcr3*^{-/-} groups of injected mice (Fig. 3a). Further,

cellular expression of IL-4 receptor and mannose receptor in these macrophage populations were comparable in both groups of mice, indicative of macrophage polarization towards the alternatively activated phenotype (Fig. 3b,c), which is generally associated with tumor progression in a number of cancer models.² Interestingly, analysis of tumors from both groups of mice via immunohistochemistry revealed greater amounts of arginase-1, an enzyme known to mediate M2 macrophage activity,³⁰ in *cxcr3*^{-/-} mice than WT mice (Fig. 3d). Further, inducible nitric oxide synthase (iNOS), which is produced mainly by M1 macrophages was less in tumors of *cxcr3*^{-/-} mice compared to WT mice (Fig. 3e). Taken together, these results suggest that macrophage polarization to the tumor promoting M2 phenotype in PyMT breast cancer tumors is enhanced in the absence of CXCR3.

Accumulation of tumor promoting myeloid derived immune cell populations in the spleens of *cxcr3*^{-/-} mice with breast cancer

Since spleens of tumor bearing mice are known to contain increased proportions of M2 macrophages,³¹ we analyzed this and other cell populations in the spleens of *cxcr3*^{-/-} and WT mice injected with PyMT breast cancer cells. Flow cytometric analysis of splenic populations revealed enhanced accumulation of F4/80^{lo} CD11b⁺ cells (P1) which express IL-4 receptor as well as F4/80^{med} CD11b⁺ cells (P2) expressing mannose receptor and IL-4 receptor in *cxcr3*^{-/-} mice compared to WT mice (Fig. 4a-d), suggestive of the phenotype associated with myeloid derived suppressor cells. Further, the accumulation of F4/80^{hi} CD11b⁺ population (P3) was enhanced in the spleens of *cxcr3*^{-/-} mice with breast cancer tumors and displayed higher surface expression of mannose receptor than WT counterparts (Fig. 4b,d), indicative of an increased M2 polarized profile. Further, mRNA expression levels of arginase-1 in the spleens of *cxcr3*^{-/-} mice were higher than in WT mice (Fig. 4e). These results demonstrate that the absence of CXCR3 promotes

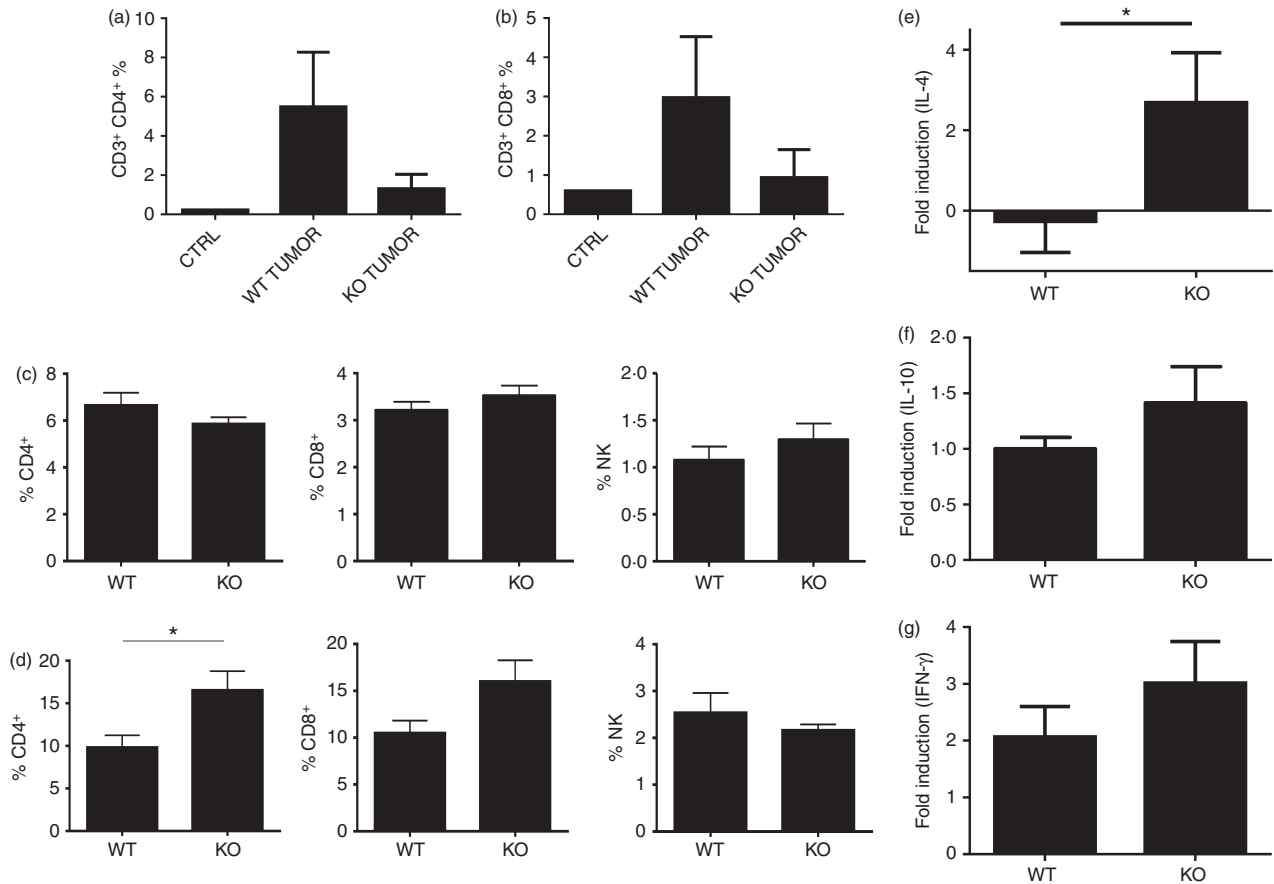


Figure 2. Frequency of tumor infiltrating lymphocytes in WT and *cxcr3*^{-/-} C57BL/6 mice injected with PyMT breast cancer cell line: (a and b) Percentages of (a) CD4⁺ and (b) CD8⁺ T cells in tumors of WT and *cxcr3*^{-/-} mice injected with PyMT cancer cells. (c and d) Percentages of CD4⁺ T cells, CD8⁺ T cells and NK cells in (c) spleens and (d) lymph nodes of WT and *cxcr3*^{-/-} mice injected with PyMT cancer cells. Data are mean values from 4 to 5 individual mice per group and are representative of three independent experiments with similar results. **P* < 0.05. (e–g) Real time PCR analysis of (e) IL-4, (f) IL-10 and (g) IFN-γ mRNA induction in tumors of WT and *cxcr3*^{-/-} mice injected with PyMT cancer cells. Data shown are mean ± SE of duplicates from four or five individual mice per group and are representative of three individual experiments. **P* < 0.05.

the accumulation and differentiation of immune cell populations in the spleen which contribute to an immune response that favors tumor growth and progression.

In vitro activation of T cells and macrophages obtained from *cxcr3*^{-/-} mice favor M2 polarization

To delineate cellular mechanisms why *cxcr3*^{-/-} mice display an increased M2 polarized immune response during PyMT breast cancer progression, we examined whether the absence of CXCR3 affects activation/differentiation of T cells and macrophages under various stimulation conditions. Although it is well established that CXCR3 ligands contribute to Th1 polarization through an IFN-γ mediated pathway, we observed that T cells from *cxcr3*^{-/-} mice produce similar amounts of IFN-γ as WT after *in vitro* activation with anti CD3 and anti CD28 antibodies (Fig. 5a). Interestingly, amounts of Th2 cytokines IL-4 and IL-10 were increased in *cxcr3*^{-/-} T cells activated with anti CD3/CD28 antibodies compared to WT

(Fig. 5b,c), while amounts of IL-13 were similar between the groups (Fig. 5d). Combined with our *in vivo* cytokine induction data in tumor injected mice, these results demonstrate that activation of *cxcr3*^{-/-} T cells result in production of cytokines that favor macrophage M2 polarization.

We further examined whether macrophages from *cxcr3*^{-/-} mice have a greater propensity towards M1 or M2 polarization compared to WT macrophages under various stimulation conditions. Cytokine and nitric oxide production as well as iNOS mRNA expression of bone marrow derived macrophages (BMDMs) from naïve WT and *cxcr3*^{-/-} mice were measured after *in vitro* stimulation with IL-4, LPS, IFN-γ or LPS/IFN-γ. Production of cytokines TNF-α, IL-6 and IL-10 by BMDMs after LPS and IFN-γ stimulation were comparable in *cxcr3*^{-/-} and WT mice (Fig. 6a). Nitric oxide production by both groups of mice was similar after LPS or LPS/IFN-γ stimulation (Fig. 6b). However, IFN-γ stimulation of BMDMs produced greater amounts of nitric oxide in WT mice

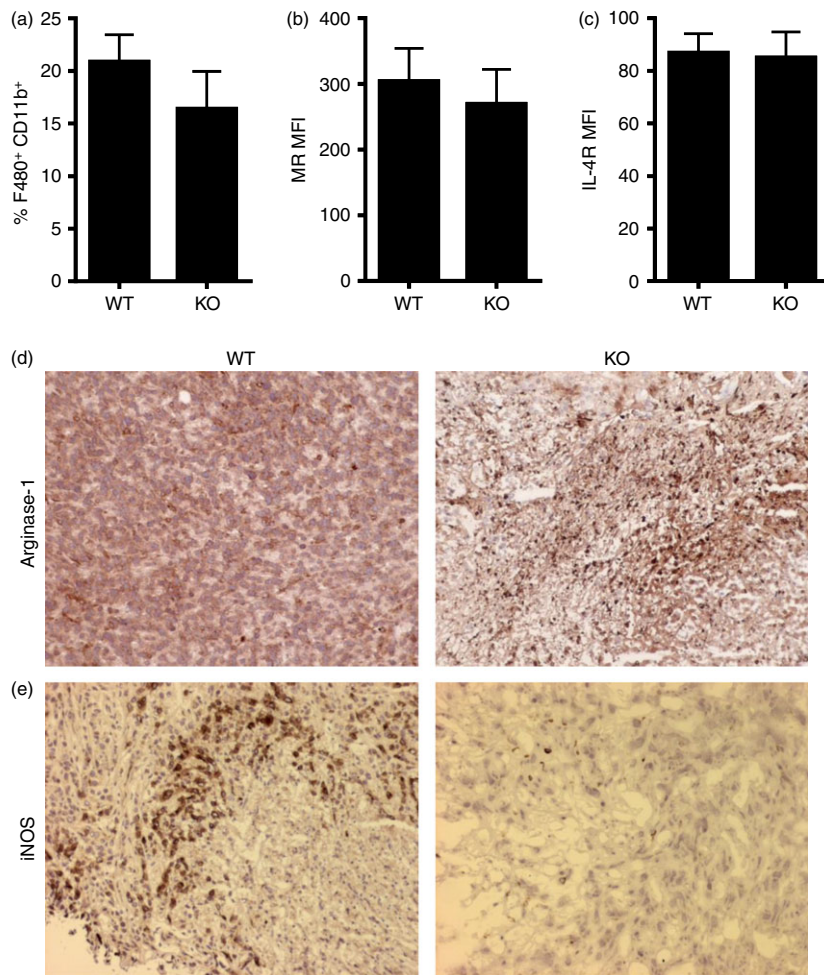


Figure 3. M2 macrophage populations are increased in *ccr3*^{-/-} mice containing tumors: (a) Frequency of F4/80⁺ CD11b⁺ macrophages in tumors of WT and *ccr3*^{-/-} mice injected with PyMT cancer cells. (b and c) Mean fluorescence intensities (MFIs) of (b) mannose receptor and (c) IL-4 receptor on F4/80⁺ CD11b⁺ macrophages in breast tumors of WT and *ccr3*^{-/-} mice injected with PyMT cells. All flow cytometric data shown are mean ± SE of four or five individual mice per group and are representative of three independent experiments. (d and e) Representative microscopic images showing immunohistochemical staining of (d) arginase-1 and (e) iNOS in breast cancer tumor sections from WT and *ccr3*^{-/-} mice injected with PyMT cells.

than in *ccr3*^{-/-} mice (Fig. 6b). Further, iNOS mRNA levels were greater in WT BMDMs stimulated with IFN- γ than in *ccr3*^{-/-} BMDMs (Fig. 6c), while IL-4 stimulation resulted in comparably enhanced induction of arginase-1 mRNA in both groups of BMDMs (Fig. 6d). These results show that the absence of CXCR3 impedes the response of BMDMs to IFN- γ stimulation and subsequent induction of iNOS and production of nitric oxide. This deficiency in IFN- γ responsiveness could play a role in the increased macrophage M2 polarization that is observed in *ccr3*^{-/-} mice.

BMDM stimulation by PyMT supernatants result in increased M2 polarization in *ccr3*^{-/-} mice

As a more relevant indicator of macrophage behavior in response to PyMT breast cancer progression, we examined BMDM responses to stimulation by PyMT supernatants *in vitro*. BMDMs from *ccr3*^{-/-} mice displayed significantly greater induction of arginase-1 mRNA after stimulation with PyMT supernatant (Fig. 6e). Conversely, levels of iNOS mRNA induction were

significantly lower in *ccr3*^{-/-} BMDMs than WT counterparts (Fig. 6f). Taken together, these results show that macrophage populations in *ccr3*^{-/-} mice display an increased tendency towards M2 polarization after *in vitro* activation under stimulation conditions potentially experienced during breast cancer development and tumor progression.

IL-4 blockade does not reduce tumor progression in *ccr3*^{-/-} mice

Our *in vivo* and *in vitro* data suggested that enhanced IL-4 production by tumor bearing *ccr3*^{-/-} mice might be a possible mechanism for the observed increase in tumor growth. We therefore determined whether blockade of IL-4 using anti-IL-4 antibody could reduce tumor progression in *ccr3*^{-/-} mice. Interestingly, tumor growth in anti-IL-4 treated *ccr3*^{-/-} mice remained similar to isotype control treated *ccr3*^{-/-} mice (Fig. 7). Our result indicates that IL-4 might play a minimal/secondary role in determining the outcome of breast cancer tumors in *ccr3*^{-/-} mice.

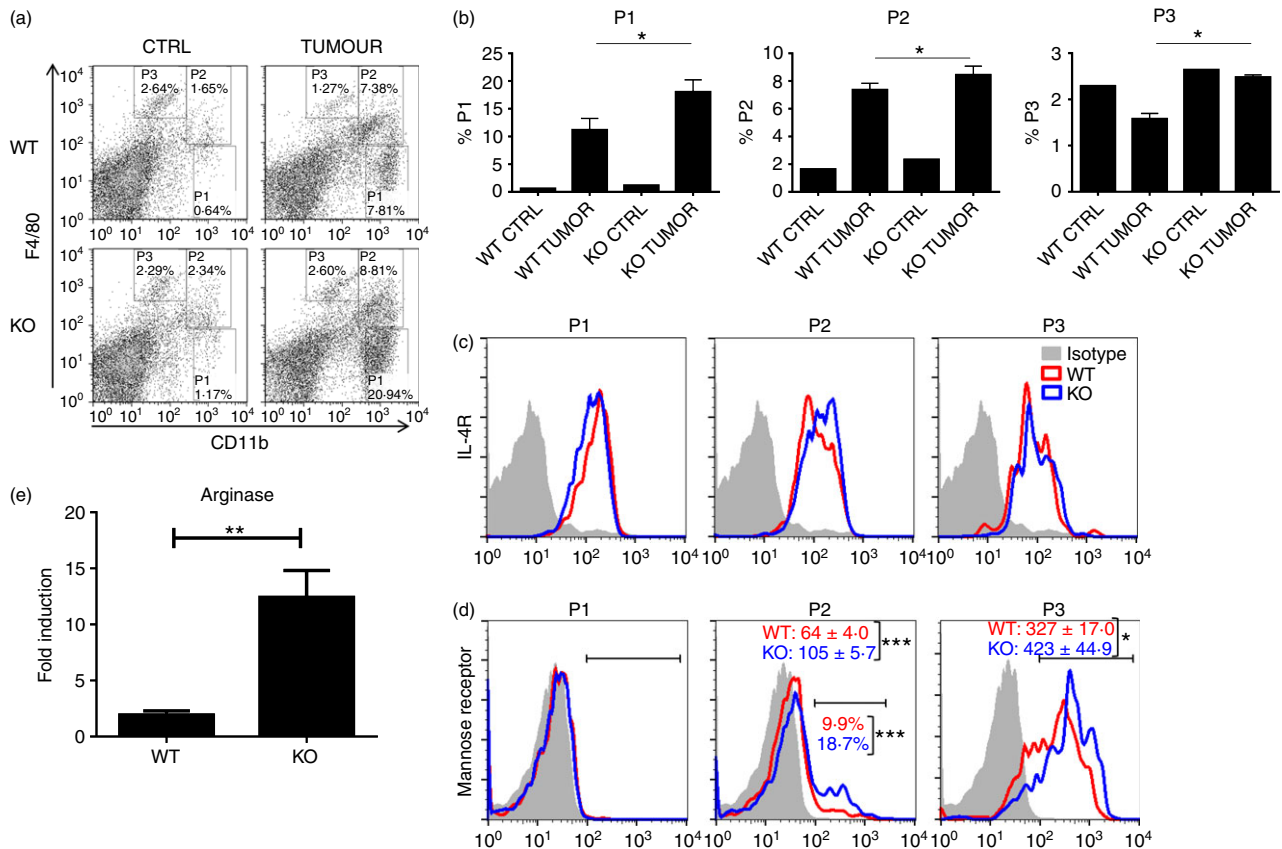


Figure 4. Accumulation of tumor promoting myeloid derived immune cell populations in the spleens of *cxcr3*^{-/-} mice with breast cancer: (a) Representative dot plots showing myeloid derived immune cell populations in the spleens of PyMT injected WT and *cxcr3*^{-/-} mice. Splenocytes were stained with CD11b, F4/80, CD206 and IL-4R. (b) Bar graph showing frequency of various myeloid derived immune cell populations in spleens of WT and *cxcr3*^{-/-} mice injected with PyMT cancer cells, based on the gating scheme depicted in Fig. a. Data shown are mean ± SE of four or five individual mice per group and are representative of three individual experiments with similar results. **P* < 0.05 (c) Representative histogram plots showing expression of IL-4 receptor on P1, P2 and P3 gated populations in spleens of WT and *cxcr3*^{-/-} mice injected with PyMT cancer cells. (d) Representative histogram plots showing expression of Mannose receptor (CD206) on P1, P2 and P3 gated populations in spleens of WT and *cxcr3*^{-/-} mice injected with PyMT cancer cells. Numbers represent average of mean fluorescence intensities (MFIs) of mannose receptor expression or percentages of mannose receptor expressing cells on gated populations. Data shown are mean ± SE of four or five individual mice per group and are representative of three independent experiments. (e) Real time PCR analysis of arginase-1 mRNA induction in spleens of PyMT injected WT and *cxcr3*^{-/-} mice ***P* < 0.01.

Discussion

Our study reveals a role for CXCR3 in the control of breast cancer tumorigenesis in an orthotopic PyMT model of breast cancer. Recent studies have shown that expression of CXCR3 promotes breast cancer metastasis^{16,32} and has been suggested as a prognostic indicator for breast cancer survival^{33,34} in patients and in some murine models. In other studies, exogenous expression of CXCR3 ligands CXCL9¹⁹ or CXCL11³⁵ have been shown to promote an anti-tumor microenvironment leading to tumor regression, and this approach has been suggested as a possible therapeutic target in breast cancer patients.²⁰ In this study, we extend the role for CXCR3 using a murine model of orthotopic breast cancer and provide evidence that the absence of the chemokine receptor CXCR3

in the host contributes to the progression of tumors in this model.

Tumor infiltrating lymphocytes (TILs) within the tumor microenvironment are essential in generating an antitumor immune response, and tumor suppressive T cells and NK cells have been shown to play a major part.^{19,36,37} In our breast cancer model, we observed slightly increased numbers of infiltrating CD4⁺ and CD8⁺ T cells in the tumors of WT than in *cxcr3*^{-/-} mice. Owing to the redundancy in chemokine receptor mediated cellular migration during inflammatory conditions, it is not surprising that CD4⁺ and CD8⁺ T cells infiltrated tumors of *cxcr3*^{-/-} mice. It was significant though, that increased levels of IL-4 mRNA were observed in tumors of *cxcr3*^{-/-} mice, suggesting greater proportions of Th2 cells in the tumor. We also observed increased IL-4 gene expression in the spleens of *cxcr3*^{-/-}

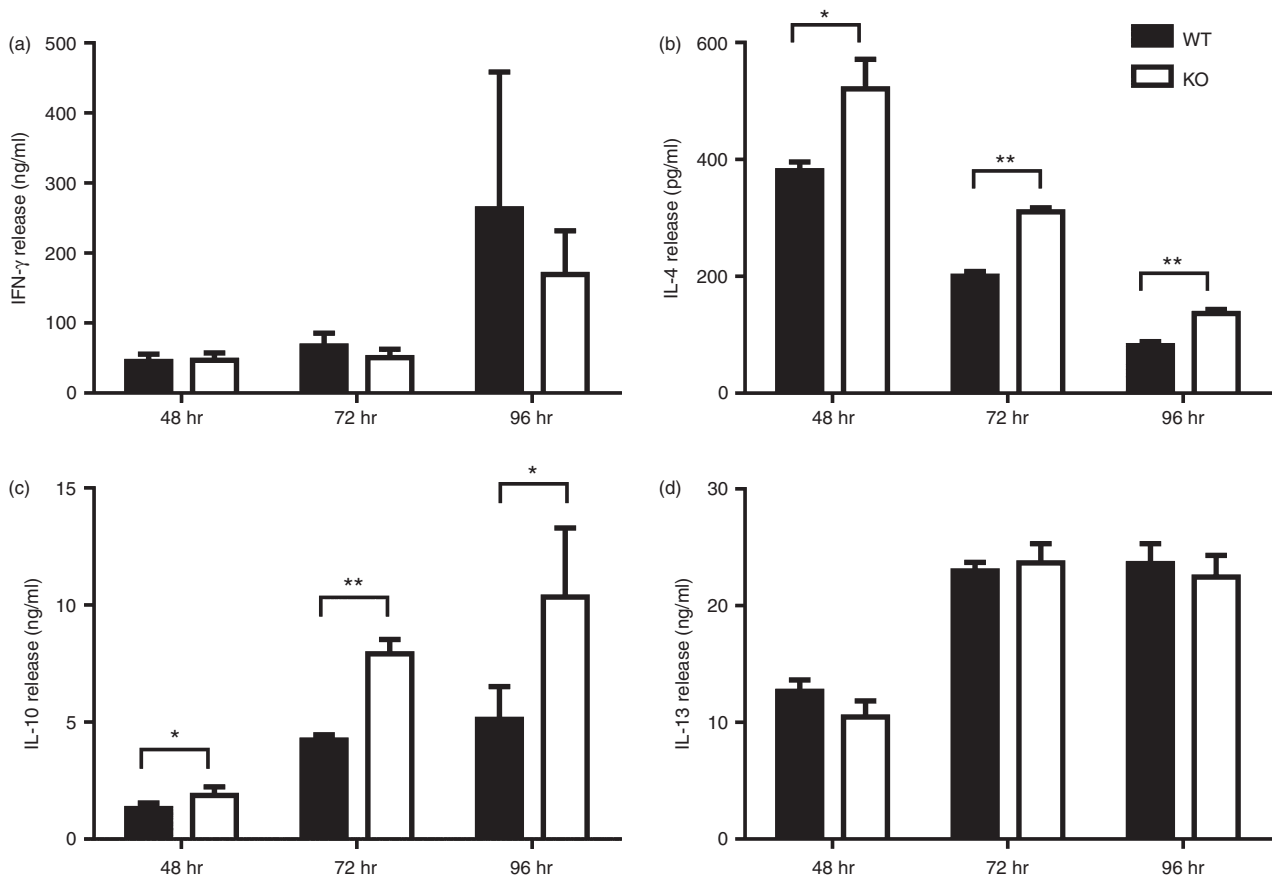


Figure 5. *In vitro* activation of T cells favor Th2 polarization in *cxcr3*^{-/-} mice: (A - D) Cytokine production of T cells from naïve WT and *cxcr3*^{-/-} mice activated with plate bound anti CD3/CD28 antibodies. (a) IFN- γ , (b) IL-4, (c) IL-10 and (d) IL-13 production were measured in culture supernatants by ELISA. Data shown are mean \pm SE of duplicates from three or four individual mice per group and are representative of two independent experiments **P* < 0.05, ***P* < 0.01.

compared to WT mice orthotopically injected with PyMT cells. In a number of cancer models, the presence of IL-4 promotes the development of tumors.^{38,39} However, in our model, *in vivo* administration of anti-IL-4 antibody did not reduce breast cancer tumors, which suggests that increased tumor growth in *cxcr3*^{-/-} mice is IL-4 independent. It could be that the absence of IL-4 is compensated for by other Th2 cytokines such as IL-13, which also signals through the IL-4 receptor and promotes alternative macrophage activation. We are undertaking additional studies to determine this possibility. Nevertheless, the inherent tendency of *cxcr3*^{-/-} macrophage polarization towards the M2 phenotype, even in the absence of IL-4, as well as their deficiency in response to IFN- γ stimulation, as demonstrated by our *in vitro* data, appears to be the predominant cause of enhanced tumor progression in *cxcr3*^{-/-} mice.

The role of tumor associated macrophage populations is well established in breast cancer.^{2,27} M2 macrophages are generally associated with tumor progression in breast cancer. As demonstrated by our immunohistochemical data and realtime PCR results, genetic deletion of CXCR3 increased M2 polarization compared to WT counterparts,

in mice orthotopically injected with PyMT cells. Similar results were observed following stimulation of *cxcr3*^{-/-} macrophages with PyMT supernatants, suggesting an intrinsic tendency towards M2 macrophage polarization in the absence of CXCR3. Further, the increased levels of IL-4 which contributes to alternative macrophage activation,⁴⁰ observed in tumors and spleens of PyMT injected *cxcr3*^{-/-} mice could amplify M2 macrophage differentiation, although this mechanism is not absolutely required.

IFN- γ stimulation of macrophages contributes to the generation of iNOS and nitric oxide which have been shown to inhibit tumor growth and progression. In *cxcr3*^{-/-} mice, the ability of macrophages to produce these factors after stimulation with IFN- γ *in vitro* was attenuated when compared to WT mice. Therefore, even though IFN- γ levels in the tumors of both groups of mice were comparable, the observed deficiency in IFN- γ responsiveness could provide another explanation for diminished antitumor responses in the absence of CXCR3. Other researchers have observed similar defects in macrophage activation when CXCR3 is deleted genetically or blocked chemically.²⁴⁻²⁶ More recently, it was shown that a disrupted

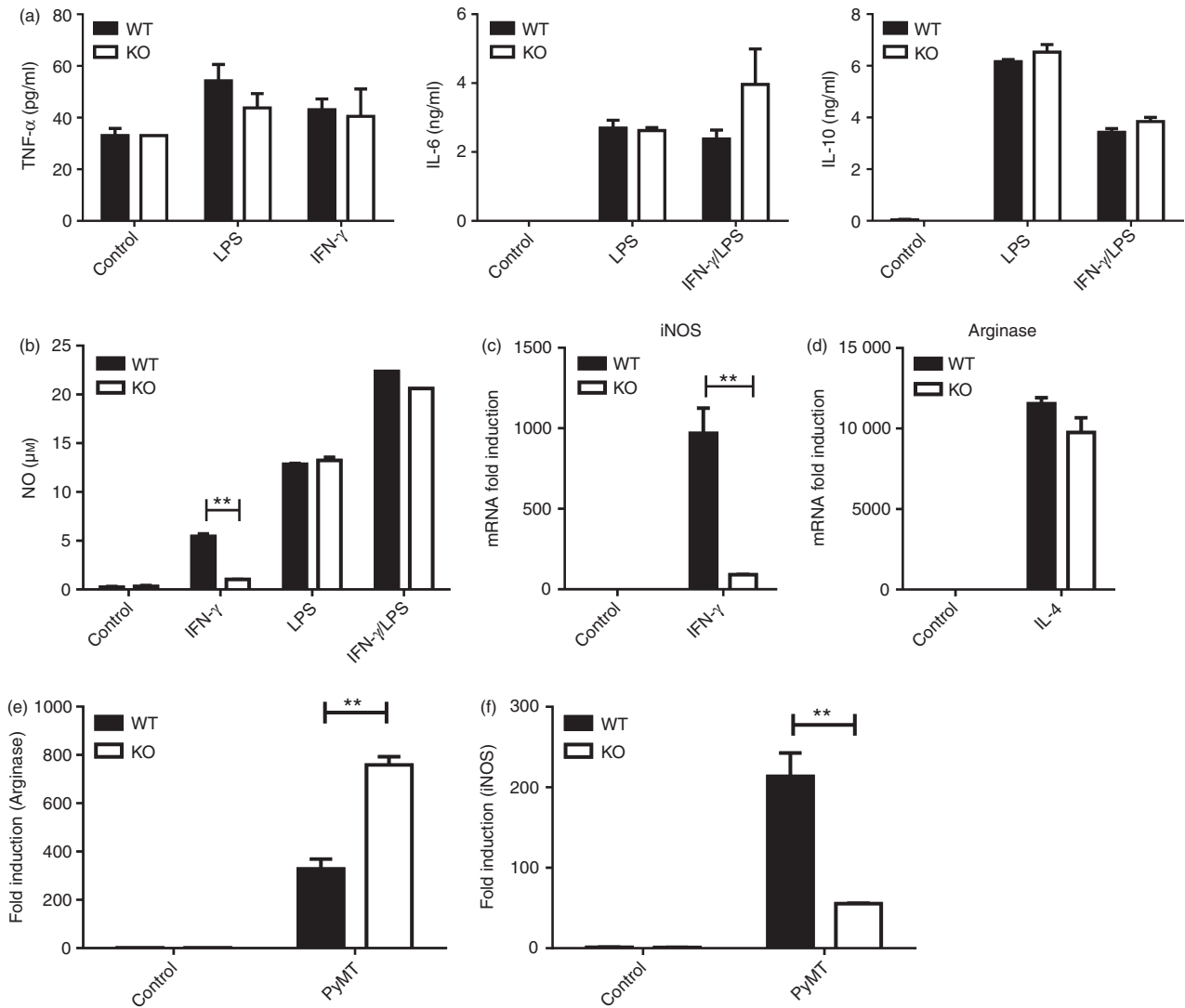


Figure 6. *In vitro* activation of macrophages favor M2 polarization in *cxcr3*^{-/-} mice: (a) Cytokine production by BMDMs from WT and *cxcr3*^{-/-} mice stimulated *in vitro* by LPS, IFN- γ and/or LPS/IFN- γ as determined by ELISA. Data shown are mean \pm SE of duplicates from three or four individual mice per group and are representative of two independent experiments. (b) Nitric oxide production by BMDMs from WT and *cxcr3*^{-/-} mice stimulated *in vitro* by IFN- γ for 48 hr, as determined by Griess reaction. (c) Real time PCR analysis of inducible nitric oxide synthase (iNOS) mRNA induction in BMDMs from naïve WT and *cxcr3*^{-/-} mice stimulated with IFN- γ . (d) Real time PCR analysis of arginase-1 mRNA induction in BMDMs from naïve WT and *cxcr3*^{-/-} mice stimulated with IL-4. (E and F) Real time PCR analysis of (e) arginase-1 and (f) iNOS mRNA induction in BMDMs from naïve WT and *cxcr3*^{-/-} mice stimulated with PyMT cancer cell culture supernatants. Data shown are mean \pm SE of duplicates from three or four individual mice per group and are representative of three independent experiments ****P* < 0.01.

IL12/IFN- γ /NO axis occurs in *cxcr3*^{-/-} macrophages.⁴¹ While the mechanism behind this altered response to IFN- γ stimulation by macrophages lacking CXCR3 is yet to be fully understood, it is possible that this is mediated by a lack of response to the CXCR3 ligands IP-10 and MIG, which are induced by IFN- γ stimulation.

Metabolic products of tumor cells play major roles in determining the outcome of a tumor challenge.⁴² Our analysis of PyMT supernatant triggered responses in BMDMs of WT and *cxcr3*^{-/-} mice revealed significantly higher levels of arginase-1 and lower levels of iNOS induction in *cxcr3*^{-/-} mice compared to WT mice.

Although components in PyMT supernatants as well as mechanisms involved in the observed differences need to be characterized, it is evident that TAMs in *cxcr3*^{-/-} mice have a much higher propensity towards M2 macrophage polarization within the tumor microenvironment of the orthotopic PyMT model of breast cancer.

In conclusion we show that *cxcr3*^{-/-} mice display increased susceptibility to breast cancer and enhanced PyMT breast tumor growth, which is likely due to increased M2 polarization in the tumors and spleens of affected mice. Identifying factors that contribute to susceptibility to breast cancer tumors provide additional targets

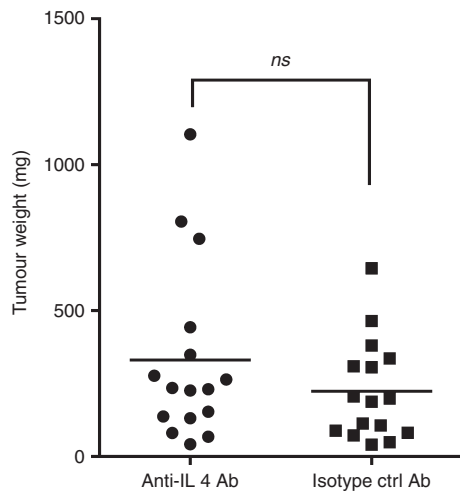


Figure 7. IL-4 blockade does not reduce tumor progression in *cxcr3*^{-/-} mice: Tumor weights of *cxcr3*^{-/-} mice treated with anti-IL-4 antibody or isotype control antibody. Tumors weights were measured 5 weeks after injection of PyMT cells. Data shown are mean values from fifteen to eighteen individual mice per group from 3 independent experiments (*ns* – not significant).

for therapeutic and vaccination strategies, which could be used in combination with other targeted approaches.²⁷ For example, forced expression of the CXCR3 ligand CXCL11 has been suggested for immunotherapeutic design strategies as it is associated with tumor regression in a murine model of breast cancer.³⁵ Pharmacologic inhibition of cyclooxygenase has been shown to increase the expression of CXCR3 ligands CXCL9 and CXCL10 which promote anti-tumor immune responses in breast cancer.²⁰ The use of CXCR3 agonists can potentially be another therapeutic approach to suppress tumor promoting Th2 cytokine production and M2 macrophage polarization which could lead to regression of breast cancer tumors.

Acknowledgements

SO, RKG and ARS conceived and designed the study, SO, SV, DK, MWN and CAP performed experiments, SO and CT analyzed data, SO and ARS wrote the manuscript. All authors reviewed and approved the final manuscript.

This work was supported by National Institute of Dental and Craniofacial Research Training Grant T32DE014320 awarded to S.O, National Institute of Health Grants CA109527 and CA153490 to R.K.G, and National Institutes of Health Grant R03AI090231 to A.R.S.

We thank Dr. Hai for providing the PyMT cells and Charles Penrose for assisting with tumor measurements.

Disclosures

The authors have no potential conflicts of interest.

References

- Sato E, Olson SH, Ahn J *et al.* Intraepithelial CD8+ tumor-infiltrating lymphocytes and a high CD8+regulatory T cell ratio are associated with favorable prognosis in ovarian cancer. *Proc Natl Acad Sci U S A* 2005; **102**:18538–43.
- Galdiero MR, Garlanda C, Jaillon S, Marone G, Mantovani A. Tumor associated macrophages and neutrophils in tumor progression. *J Cell Physiol* 2013; **228**: 1404–12.
- Menard S, Tomasic G, Casalini P *et al.* Lymphoid infiltration as a prognostic variable for early-onset breast carcinomas. *Clin Cancer Res* 1997; **3**:817–9.
- DeNardo DG, Coussens LM. Inflammation and breast cancer. Balancing immune response: crosstalk between adaptive and innate immune cells during breast cancer progression. *Breast Cancer Res* 2007; **9**:212.
- Sica A, Mantovani A. Macrophage plasticity and polarization: in vivo veritas. *J Clin Invest* 2012; **122**:787–95.
- Hagemann T, Wilson J, Burke F *et al.* Ovarian cancer cells polarize macrophages toward a tumor-associated phenotype. *J Immunol* 2006; **176**:5023–32.
- Laoui D, Movahedi K, Van Overmeire E *et al.* Tumor-associated macrophages in breast cancer: distinct subsets, distinct functions. *Int J Dev Biol* 2011; **55**:861–7.
- Groom JR, Luster AD. CXCR3 ligands: redundant, collaborative and antagonistic functions. *Immunol Cell Biol* 2011; **89**:207–15.
- Oghumu S, Lezama-Davila CM, Isaac-Marquez AP, Satoskar AR. Role of chemokines in regulation of immunity against leishmaniasis. *Exp Parasitol* 2010; **126**:389–96.
- Carr DJ, Wuest T, Ash J. An increase in herpes simplex virus type 1 in the anterior segment of the eye is linked to a deficiency in NK cell infiltration in mice deficient in CXCR3. *J Interferon Cytokine Res* 2008; **28**:245–51.
- Vandercappellen J, Van Damme J, Struyf S. The role of CXC chemokines and their receptors in cancer. *Cancer Lett* 2008; **267**:226–44.
- Rosas LE, Barbi J, Lu B, Fujiwara Y, Gerard C, Sanders VM, Satoskar AR. CXCR3^{-/-} mice mount an efficient Th1 response but fail to control Leishmania major infection. *Eur J Immunol* 2005; **35**:515–23.
- Mohan K, Issekutz TB. Blockade of chemokine receptor CXCR3 inhibits T cell recruitment to inflamed joints and decreases the severity of adjuvant arthritis. *J Immunol* 2007; **179**:8463–9.
- Campanella GS, Tager AM, El Khoury JK, Thomas SY, Abrzinski TA, Manice LA, Colvin RA, Luster AD. Chemokine receptor CXCR3 and its ligands CXCL9 and CXCL10 are required for the development of murine cerebral malaria. *Proc Natl Acad Sci U S A* 2008; **105**:4814–9.
- Lord GM, Rao RM, Choe H, Sullivan BM, Lichtman AH, Lusinskas FW, Glimcher LH. T-bet is required for optimal proinflammatory CD4+ T-cell trafficking. *Blood* 2005; **106**:3432–9.
- Ma X, Norsworthy K, Kundu N *et al.* CXCR3 expression is associated with poor survival in breast cancer and promotes metastasis in a murine model. *Mol Cancer Ther* 2009; **8**:490–8.
- Liu C, Luo D, Reynolds BA *et al.* Chemokine receptor CXCR3 promotes growth of glioma. *Carcinogenesis* 2011; **32**:129–37.
- Wendel M, Galani IE, Suri-Payer E, Cerwenka A. Natural killer cell accumulation in tumors is dependent on IFN- γ and CXCR3 ligands. *Cancer Res* 2008; **68**:8437–45.
- Walser TC, Ma X, Kundu N, Dorsey R, Goloubeva O, Fulton AM. Immune-mediated modulation of breast cancer growth and metastasis by the chemokine Mig (CXCL9) in a murine model. *J Immunother* 2007; **30**:490–8.
- Bronger H, Kraeft S, Schwarz-Boeger U, Cerny C, Stockel A, Avril S, Kiechle M, Schmitt M. Modulation of CXCR3 ligand secretion by prostaglandin E2 and cyclooxygenase inhibitors in human breast cancer. *Breast Cancer Res* 2012; **14**:R30.
- Taub DD, Lloyd AR, Conlon K *et al.* Recombinant human interferon-inducible protein 10 is a chemoattractant for human monocytes and T lymphocytes and promotes T cell adhesion to endothelial cells. *J Exp Med* 1993; **177**:1809–14.
- Luster AD, Greenberg SM, Leder P. The IP-10 chemokine binds to a specific cell surface heparan sulfate site shared with platelet factor 4 and inhibits endothelial cell proliferation. *J Exp Med* 1995; **182**:219–31.
- Luster AD, Leder P. IP-10, a -C-X-C- chemokine, elicits a potent thymus-dependent antitumor response in vivo. *J Exp Med* 1993; **178**:1057–65.
- Zhou J, Tang PCY, Qin L *et al.* CXCR3-dependent accumulation and activation of perivascular macrophages is necessary for homeostatic arterial remodeling to hemodynamic stresses. *J Exp Med* 2010; **207**:1951–66.
- Kakuta Y, Okumi M, Miyagawa S *et al.* Blocking of CCR5 and CXCR3 suppresses the infiltration of macrophages in acute renal allograft rejection. *Transplantation* 2012; **93**:24–31.
- Cuenca AG, Wynn JL, Kelly-Scumpia KM *et al.* Critical role for CXC Ligand 10/CXC receptor 3 signaling in the murine neonatal response to sepsis. *Infect Immun* 2011; **79**:2746–54.
- Tang X, Mo C, Wang Y, Wei D, Xiao H. Anti-tumour strategies aiming to target tumour-associated macrophages. *Immunology* 2013; **138**:93–104.

- 28 Wolford CC, McConoughey SJ, Jalgaonkar SP *et al.* Transcription factor ATF3 links host adaptive response to breast cancer metastasis. *J Clin Invest* 2013; **123**:2893–906.
- 29 Nasser MW, Qamri Z, Deol YS *et al.* S100A7 enhances mammary tumorigenesis through upregulation of inflammatory pathways. *Cancer Res* 2012; **72**:604–15.
- 30 Mills CD. Macrophage arginine metabolism to ornithine/urea or nitric oxide/citrulline: a life or death issue. *Crit Rev Immunol* 2001; **21**:399–425.
- 31 Doedens AL, Stockmann C, Rubinstein MP *et al.* Macrophage expression of hypoxia-inducible factor-1 alpha suppresses T-cell function and promotes tumor progression. *Cancer Res* 2010; **70**:7465–75.
- 32 Razmkhah M, Jaberipour M, Safaei A, Talei AR, Erfani N, Ghaderi A. Chemokine and chemokine receptors: a comparative study between metastatic and nonmetastatic lymph nodes in breast cancer patients. *Eur Cytokine Netw* 2012; **23**:72–7.
- 33 Wu Z, Han X, Yan J *et al.* The prognostic significance of chemokine receptor CXCR3 expression in colorectal carcinoma. *Biomed Pharmacother* 2012; **66**:373–7.
- 34 Li L, Chen J, Lu ZH, Yu SN, Luo YF, Zhao WG, Ma YH, Jia CW. [Significance of chemokine receptor CXCR3 expression in breast cancer]. *Zhonghua Bing Li Xue Za Zhi* 2011; **40**:85–8.
- 35 Chu Y, Yang X, Xu W, Wang Y, Guo Q, Xiong S. In situ expression of IFN-gamma-inducible T cell alpha chemoattractant in breast cancer mounts an enhanced specific anti-tumor immunity which leads to tumor regression. *Cancer Immunol Immunother* 2007; **56**:1539–49.
- 36 Cozar JM, Canton J, Tallada M, Concha A, Cabrera T, Garrido F, Ruiz-Cabello Osuna F. Analysis of NK cells and chemokine receptors in tumor infiltrating CD4 T lymphocytes in human renal carcinomas. *Cancer Immunol Immunother* 2005; **54**:858–66.
- 37 Kajitani K, Tanaka Y, Arihiro K, Kataoka T, Ohdan H. Mechanistic analysis of the anti-tumor efficacy of human natural killer cells against breast cancer cells. *Breast Cancer Res Treat* 2012; **134**:139–55.
- 38 Kammertoens T, Qin Z, Briesemeister D, Bendelac A, Blankenstein T. B-cells and IL-4 promote methylcholanthrene-induced carcinogenesis but there is no evidence for a role of T/NKT-cells and their effector molecules (Fas-ligand, TNF- α , perforin). *Int J Cancer* 2012; **131**:1499–508.
- 39 Koller FL, Hwang DG, Dozier EA, Fingleton B. Epithelial interleukin-4 receptor expression promotes colon tumor growth. *Carcinogenesis* 2010; **31**:1010–7.
- 40 Martinez FO, Helming L, Milde R *et al.* Genetic programs expressed in resting and IL-4 alternatively activated mouse and human macrophages: similarities and differences. *Blood* 2013; **121**:e57–69.
- 41 Deiluiis JA, Oghumu S, Duggineni D *et al.* CXCR3 modulates obesity-induced visceral adipose inflammation and systemic insulin resistance. *Obesity (Silver Spring)* 2013. doi: 10.1002/oby.20642
- 42 Liu Y, Chen K, Wang C, Gong W, Yoshimura T, Liu M, Wang JM. Cell surface receptor FPR2 promotes antitumor host defense by limiting M2 polarization of macrophages. *Cancer Res* 2013; **73**:550–60.